AIP | Applied Physics Letters

Effect of spin relaxation rate on the interfacial spin depolarization in ferromagnet/oxide/semiconductor contacts

Kun-Rok Jeon, Byoung-Chul Min, Youn-Ho Park, Young-Hun Jo, Seung-Young Park et al.

Citation: Appl. Phys. Lett. **101**, 022401 (2012); doi: 10.1063/1.4733478
View online: http://dx.doi.org/10.1063/1.4733478
View Table of Contents: http://apl.aip.org/resource/1/APPLAB/v101/i2
Published by the American Institute of Physics.

Related Articles

Highly (111)-oriented Ge thin films on insulators formed by Al-induced crystallization
Appl. Phys. Lett. 101, 072106 (2012)

Correlation between Ga-O signature and midgap states at the Al2O3/In0.53Ga0.47As interface
Appl. Phys. Lett. 101, 063504 (2012)

A silicon-on-insulator complementary-metal-oxide-semiconductor compatible flexible electronics technology
Appl. Phys. Lett. 101, 052106 (2012)

Generation of very fast states by nitridation of the SiO2/SiC interface
J. Appl. Phys. 112, 024520 (2012)

Quantitative investigations of aggregate systems
J. Chem. Phys. 137, 044311 (2012)

Additional information on Appl. Phys. Lett.

Journal Homepage: http://apl.aip.org/
Journal Information: http://apl.aip.org/about/about_the_journal
Top downloads: http://apl.aip.org/features/most_downloaded
Information for Authors: http://apl.aip.org/authors

ADVERTISEMENT

Effect of spin relaxation rate on the interfacial spin depolarization in ferromagnet/oxide/semiconductor contacts

Kun-Rok Jeon,[1] Byoung-Chul Min,[2] Youn-Ho Park,[2] Young-Hun Jo,[3] Seung-Young Park,[3] Chang-Yup Park,[1] and Sung-Chul Shin[1,4]
[1]*Korea Advanced Institute of Science and Technology (KAIST), Daejeon 305-701, South Korea*
[2]*Korea Institute of Science and Technology (KIST), Seoul 136-791, South Korea*
[3]*Korea Basic Science Institute (KBSI), Daejeon 305-764, South Korea*
[4]*Daegu Gyeongbuk Institute of Science and Technology (DGIST), Daegu 711-873, South Korea*

(Received 5 April 2012; accepted 20 June 2012; published online 9 July 2012)

Combined measurements of normal and inverted Hanle effects in CoFe/MgO/semiconductor (SC) contacts reveal the effect of spin relaxation rate on the interfacial spin depolarization (ISD) from local magnetic fields. Despite the similar ferromagnetic electrode and interfacial roughness in both CoFe/MgO/Si and CoFe/MgO/Ge contacts, we have observed clearly different features of the ISD depending on the host SC. The precession and relaxation of spins in different SCs exposed to the local fields from more or less the same ferromagnets give rise to a notably different ratio of the inverted Hanle signal to the normal one. A model calculation of the ISD, considering the spin precession due to the local field and the spin relaxation in the host SC, explains the temperature and bias dependence of the ISD consistently. © *2012 American Institute of Physics*. [http://dx.doi.org/10.1063/1.4733478]

The electrical injection and detection of spin-polarized carriers in semiconductors (SCs) has been successfully achieved by employing spin tunnel contacts.[1–15] However, many aspects of the spin phenomena in these systems,[1–13,16] e.g., (i) the location, magnitude, and sign of the induced spin accumulation, (ii) the unusual bias and temperature-dependence of the spin signal, and (iii) the unexpected short spin lifetime and its weak variation with temperature, require additional investigation.

Recently, Dash *et al.* have shown the effect of local-field strength on the spin signals in ferromagnet (FM)/oxide/SC contacts; it was found that the local magnetostatic fields (B_L^{ms}) arising from the finite roughness of the FM/oxide interface dramatically alter and even dominate the accumulation and dynamics of the spins in SCs.[17] Because this interfacial spin depolarization (ISD) due to B_L^{ms} is deeply interconnected with (i), (ii), and (iii),[17] a systematic study of the ISD is crucial for a complete understanding of the spin accumulation and spin dynamics in SC near FM interface. The inverted Hanle effect due to local-fields had been extensively studied in Ref. 17, using the FM/Al_2O_3/Si contacts with the same host SC but different FMs.[17] FM/Al_2O_3/GaAs contacts also showed a similar signature of the ISD with slightly different details, suggesting that the ISD is universal for the three-terminal Hanle (TTH) experiments.[17]

In this vein, it is of interest to investigate the role of host SCs on the ISD in FM/oxide/SC contacts. Here we report, using the FM/oxide/SC contacts with the same FM but different host SCs, the effect of spin relaxation rate on the ISD. The combined measurements of normal and inverted Hanle effects over wide temperature (T) and bias current (I) range[18] reveal the effect of spin relaxation rate on the ISD in CoFe/MgO/Si and CoFe/MgO/Ge contacts. We have observed, despite more or less the same ferromagnetic electrode and the interfacial roughness of the FM/oxide/SC contacts, significant differences of the ISD depending on the host SC; the spin accumulation in different SCs exposed to the local fields from similar FMs gives rise to a clearly different ratio of the inverted Hanle signal to the normal one. This can be understood in terms of two competing mechanisms in the host SCs, namely, the spin relaxation and spin precession due to the local fields.

Two types of CoFe(5 nm)/MgO(2 nm)/n-SC(001) tunnel contacts were prepared using a molecular beam epitaxy system. The first one is a highly ordered CoFe/MgO/Si contact where the Si channel is a heavily As-doped ($n_d \sim 2.5 \times 10^{19}\text{cm}^{-3}$ at 300 K),[6] and the second one is a single-crystalline CoFe/MgO/Ge contact where the Ge channel consists of a heavily P-doped surface layer ($n_d \sim 10^{19}\text{cm}^{-3}$ at 300 K) and a moderately Sb-doped substrate ($n_d \sim 10^{18}\text{cm}^{-3}$ at 300 K).[10] In order to measure the induced spin accumulation ($\Delta\mu = \mu^{\uparrow} - \mu^{\downarrow}$) in the spin tunnel contacts, we have fabricated devices for the TTH measurements,[1–4] consisting of multiple CoFe/MgO/n-SC tunnel contacts ($100 \times 100\ \mu\text{m}^2$). Details of the sample preparation as well as the structural and electrical characterization are available in the literature.[6,10,19] It should be noted that the dominant transport mechanism for both CoFe/MgO/Si and CoFe/MgO/Ge contacts is tunneling, as proven by the symmetric I-V curve and its weak temperature-dependence; the both types of contacts reveal the narrow depletion region of ~5 nm and the small resistance-area values ($\sim 5 \times 10^{-6}\ \Omega\text{m}^2$ (300 K) to $\sim 1 \times 10^{-5}\ \Omega\text{m}^2$ (5 K) at −0.25 V).[6,10]

To estimate the magnitude of B_L^{ms}, which scales with the roughness of the FM interface and the magnetization of the FM,[17] we have characterized the roughness of an MgO/SC reference structure without FM using atomic force microscopy (AFM) and magnetic property of complete FM/MgO/SC structures using vibrating sample magnetometry (VSM). The MgO/SC reference structure show a root-mean-square (RMS) roughness of ~0.2 nm, peak-to-peak height

variations of ~0.3–0.4 nm, and lateral correlation lengths of 30–50 nm. The FM/MgO/SC samples have saturation magnetization (M_s) values of ~1400–1430 emu/cc with a normalized remanence (M_r/M_s, where M_r is remanent magnetization) of ~0.93–0.95 for the easy axis magnetization. Because the depletion region width of both CoFe/MgO/Si and CoFe/MgO/Ge contacts are more or less the same (about 5 nm),[6,10] the locations of spin accumulation in both contacts are likely to be similar to each other. Taking into account the similar roughness, magnetization, and depletion width, it is likely that the magnitude of B_L^{ms} at the interface is not fundamentally different in both CoFe/MgO/Si and CoFe/MgO/Ge contacts.

Using the CoFe/MgO/Si and CoFe/MgO/Ge contacts, we have conducted high-field TTH measurements (up to ±3 T) under perpendicular ($M \perp B$, closed circles) and in-plane ($M//B$, open circles) magnetic field (Fig. 1). The TTH measurements show the overall behavior of the spin accumulation signals as a function of external magnetic fields ($B_\perp$, $B_{//}$). The control experiments[9] using a nonmagnetic interlayer[20] confirm that the observed Hanle signals in our system are originated from the spin accumulation.

As indicated in Fig. 1, three distinct regions were observed in the $M \perp B$ measurements (closed circles): (i) the Hanle effect at small magnetic fields, (ii) the rotation of magnetization (M), and (iii) the saturation of M. As $B_\perp$ is increased, the voltage signal from the spin accumulation is sharply reduced due to the Hanle effect in region (i), and thereafter it gradually increases when the M of the FM rotates out of the plane in region (ii). When the M and induced spin accumulation in the SC are fully aligned with $B_\perp$ higher than the demagnetization field (~2.2 T) of CoFe, the voltage signal eventually becomes saturated in region (iii). Both CoFe/MgO/Si and CoFe/MgO/Ge contacts show a very similar field dependence of spin signals in the $M \perp B$ measurements.

On the other hand, the $M//B$ measurement (open circles) shows a clear difference in the field dependence of spin signals between the CoFe/MgO/Si and CoFe/MgO/Ge contacts. We have observed a sizable inverted Hanle effect[17] in the CoFe/MgO/Si contact. At zero or small external magnetic fields, the injected spins are precessed and dephased by local magnetostatic fields having random directions, which result in a reduction of the spin accumulation.[17] In contrast, a larger external magnetic field ($B_{//}$) can eliminate the local magnetostatic fields, restoring a full spin accumulation.[17] The overall behavior of the voltage signals (for the perpendicular and in-plane field) is in good agreement with the findings of the previous study on FM/Al_2O_3/SC tunnel contacts.[17]

In the $M//B$ measurement, the CoFe/MgO/Ge contact shows two clear differences from the CoFe/MgO/Si contact. First, the spin signals in the saturation region (iii) are significantly different in the $M \perp B$ and $M//B$ measurements. This is a consequence of the tunneling anisotropic magnetoresistance (TAMR)[21–25]; the tunnel resistance depends on the angle between the M and crystal axes of FM because the tunneling electrons experience the anisotropic density of states with respect to M via the spin-orbit interaction. The effect of TAMR on the spin signals has been also observed in the Fe/MgO/Ge and Co/Al_2O_3/GaAs tunnel contacts.[8,17] The positive background signal in the CoFe/MgO/Ge contact may be ascribed to the Lorentz MR (LMR) in Ge substrate due to its high mobility (note that the LMR is quadratic in mobility). The second difference between two contacts is that the CoFe/MgO/Ge contact has a small magnitude of the inverted Hanle effect. Considering that the injected spins experience a similar magnitude of B_L^{ms}, the difference in the magnitude of the in-plane Hanle signal is rather unexpected.

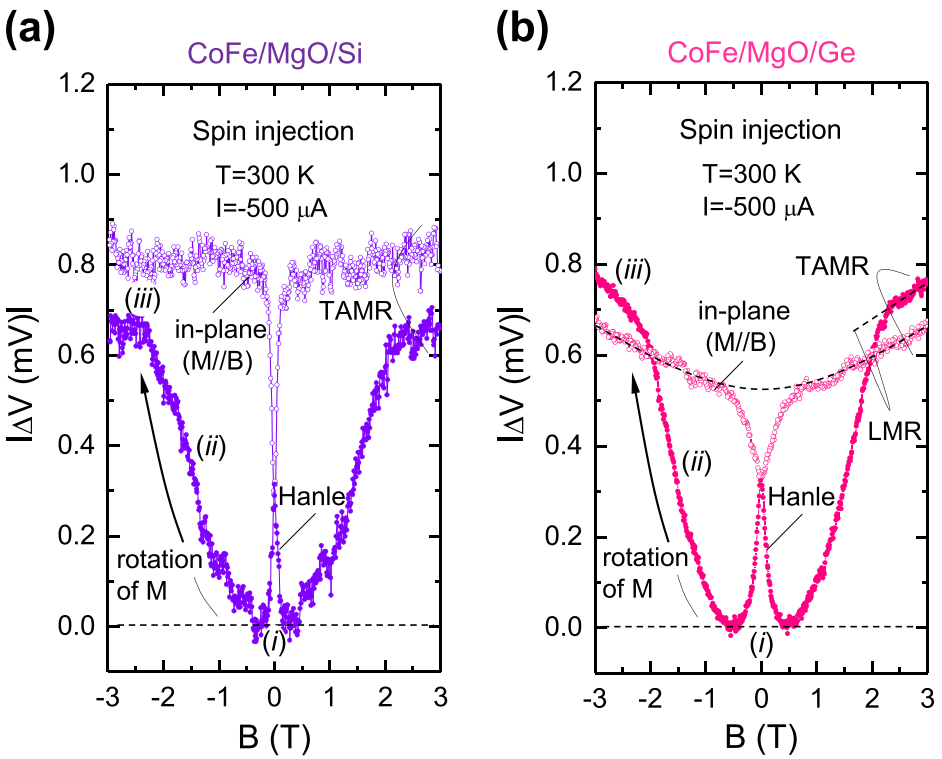

FIG. 1. High-field Hanle measurements (up to ±3 T) on (a) CoFe/MgO/Si and (b) the CoFe/MgO/Ge contacts at 300 K under perpendicular ($M \perp B$, closed circles) and in-plane ($M//B$, open circles) measurement schemes.

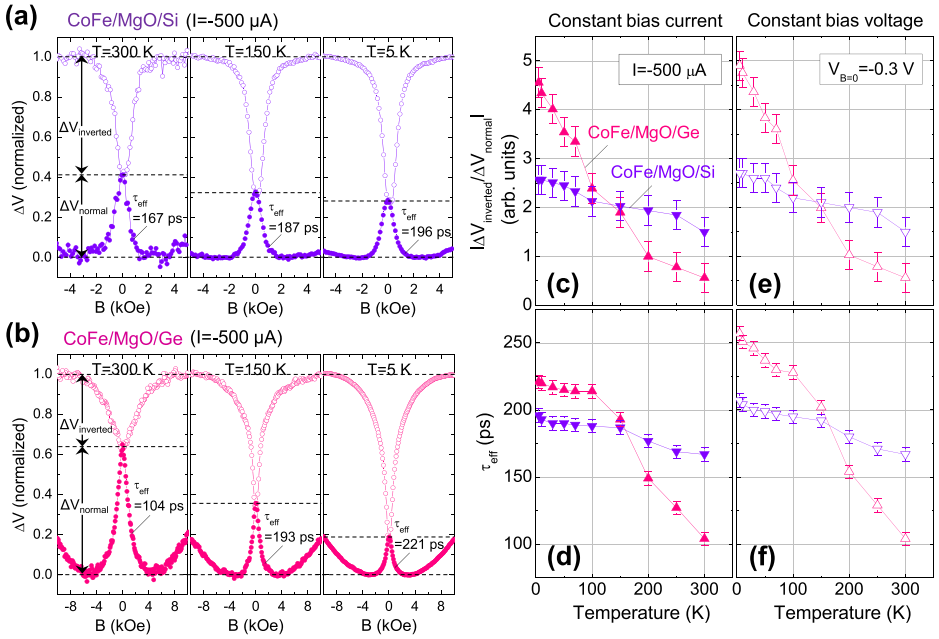

FIG. 2. Normal (ΔV_{normal}) and inverted ($\Delta V_{inverted}$) Hanle effects on (a) CoFe/MgO/Si and (b) CoFe/MgO/Ge contacts under $M \perp B$ (closed circles) and $M // B$ (open circles) measurements, respectively, at an applied current (I) of $-500\,\mu$A (spin injection condition) for various temperatures. (c) Interfacial spin depolarization effect ($|\Delta V_{inverted}/\Delta V_{normal}|$) and (d) effective spin lifetime (τ_{eff}) as a function of the temperature (T) at the constant bias current (I) of $-500\,\mu$A. (e) $|\Delta V_{inverted}/\Delta V_{normal}|$ and (f) τ_{eff} with T at the constant bias voltage ($V_{B=0}$) of -0.3 V.

The spin injection under the random B_L^{ms} results in the precession of injected spins with an angular frequency of $\omega_L^{ms} = g\mu_B B_L^{ms}/\hbar$, where g is the Landé g-factor, μ_B is the Bohr magneton, and $\hbar$ is the Planck constant divided by 2π. Accompanying the spin precession in random orientation, the spin relaxation with a spin lifetime of τ_{sf} takes place as a consequence of the microscopic spin scatterings inside the SC. If $\tau_{sf} \ll 1/\omega_L^{ms}$, the spins are completely relaxed within their spin lifetime before being precessed by B_L^{ms}. In this case, the suppression of spin accumulation by B_L^{ms} is negligible, leading to a small $|\Delta V_{inverted}/\Delta V_{normal}|$. In contrast, if $\tau_{sf} \geq 1/\omega_L^{ms}$, the $|\Delta V_{inverted}/\Delta V_{normal}|$ becomes pronounced because the spins are precessed many times in B_L^{ms} and randomized within their τ_{sf}, resulting in the sizable suppression of the spin polarization by B_L^{ms}.

Here we define $R_{ISD} \equiv |\Delta V_{inverted}/\Delta V_{normal}|$, the ratio of the inverted Hanle signal to the normal one, which is quite a good measure of the ISD in CoFe/MgO/SC contacts. Despite the similar magnitude of B_L^{ms}, the inverted Hanle signals in Fig. 1 clearly show that the R_{ISD} is more pronounced for the CoFe/MgO/Si contact than it is for the CoFe/MgO/Ge contact at 300 K.

The effective strength of B_L^{ms} for spins located 7 nm away from the FM interface is about 0.1–1 kOe,[17] corresponding to a $1/\omega_L^{ms}$ value of about 0.09–0.9 ns for Si ($g = 2$) and 0.11–1.1 ns for Ge ($g = 1.6$). The τ_{sf} estimated from the spin scattering via the Elliot-Yafet (EY) mechanism[26–28] is about 1 ns for heavily doped Si at 300 K. Because this τ_{sf} is comparable to $1/\omega_L^{ms}$, a large R_{ISD} can be expected for the CoFe/MgO/Si contact. If the τ_{sf} in Ge at 300 K is small due to the non-negligible spin-orbit interaction or other scattering mechanisms, the relatively weak R_{ISD} in the CoFe/MgO/Ge contact at 300 K can be explained.

The interpretation above appears even more convincing given the strong enhancement of the R_{ISD} with temperature (T). Figures 2(a) and 2(b) show the normal (ΔV_{normal}) and inverted ($\Delta V_{inverted}$) Hanle effects on the CoFe/MgO/Si and CoFe/MgO/Ge contacts under $M \perp B$ (closed circles) and $M // B$ (open circles) measurements, respectively, at an applied current (I) of $-500\,\mu$A (spin injection condition) with various temperatures. All curves are normalized by the voltage difference between the minimum value of the normal Hanle curve and the saturation value of the inverted Hanle curve in the region (i) (see Fig. 1). The magnitude of the inverted Hanle effect of the CoFe/MgO/Ge contact has been measured by excluding the background LMR effect.

From the Lorentzian fit of the Hanle curves, we can determine the effective τ_{sf} (τ_{eff}) of accumulated spins. It is difficult to extract the true or real τ_{sf} from the Hanle curve (with the Lorentzian fit) due to the artificial broadening caused by the ISD. Nevertheless, the effective value of τ_{sf} (or τ_{eff}), which should be considered as a lower bound for τ_{sf}, can be deduced. For a quantitative comparison, we have plotted the R_{ISD} and τ_{eff} as a function of T in Figs. 2(c) and 2(d), respectively.

As T decreases from 300 K to 5 K, the R_{ISD} becomes larger and the τ_{eff} increases gradually; the R_{ISD} for the CoFe/MgO/Si contact is continually enhanced ~2 times; the increase of R_{ISD} for the CoFe/MgO/Ge contact is even more pronounced; the R_{ISD} is increased ~9 times (Fig. 2(c)). Qualitatively the same behavior was observed in the T dependences of R_{ISD} and τ_{eff} obtained at the constant bias voltage ($V_{B=0}$) of -0.3 V (spin injection condition) in Figs. 2(e) and 2(f). Taking into account that $B_L^{ms}(T) \propto (1 - \alpha T^{3/2})$ with $\alpha = 3.2 \times 10^{-5}\,K^{-3/2}$ for a CoFe,[29,30] the ω_L^{ms} is slightly increased with decreasing T. It is clear that the large enhancement of the R_{ISD} at low T is mainly originated from the increase of τ_{sf}, as expected in the EY mechanism.[25–27] The temperature dependence of R_{ISD} corresponding to the τ_{eff} variation supports the interpretation based on two competing mechanisms in the host SCs, namely, the spin relaxation and spin precession due to the local fields.

Using the model in Ref. 17, we have calculated the effect of τ_{sf} on the Hanle curves with a fixed value of $1/\omega_L^{ms}$. According to the model,[17] the S_x component of steady state spin polarization $\vec{S}$ at the interface, which is parallel to the M vector of FM detector, in the presence of

local magnetostatic field (B_L^{ms}) and external applied magnetic field (B^{ext}) is expressed as

$$S_x = S_{0x}\left\{\frac{\omega_x^2}{\omega_L^2} + \left(\frac{\omega_y^2+\omega_z^2}{\omega_L^2}\right)\left(\frac{1}{1+(\omega_L\tau_{sf})^2}\right)\right\}, \quad (1)$$

where S_{0x} is the spin polarization without any magnetic field, $\omega_L^2 = \omega_x^2+\omega_y^2+\omega_z^2$, and $\omega_i = \omega_i^{ext}+\omega_i^{ms}(x,y,z)$. Here, $\omega_i^{ms}(x,y,z)$ was taken to have a periodic spatial variation with $\omega_L^{ms}\cos(2\pi x/\lambda)$, where $\omega_L^{ms} \approx 3\,\mathrm{ns}^{-1}$ (or $1/\omega_L^{ms} \approx 0.33\,\mathrm{ns}$, corresponding to a B_L^{ms} value of 0.3 kOe) and $\lambda = 40\,\mathrm{nm}$ and where the spin polarization was averaged in space over a full period λ for simplicity.

Figures 3(a)–3(c) show the calculated normal ($M\perp B$) and inverted ($M//B$) Hanle curves, which qualitatively reproduce the experimental results. As τ_{sf} is increased (with a fixed value of $1/\omega_L^{ms} \approx 0.33$ ns), the inverted Hanle effect (brown symbols) becomes pronounced; the R_{ISD} has been also increased; the widths of the normal Hanle curve (wine symbols) and inverted Hanle curve are broadened in comparison with the ideal Hanle curve (blue symbols) without B_L^{ms}.

We have also calculated the R_{ISD} as a function of τ_{sf} with the four different $1/\omega_L^{ms}$ values of 0.10, 0.33, 1.00, and ∞ ns (corresponding to B_L^{ms} values of about 1.0, 0.3, 0.1, and 0.0 kOe, respectively)

$$R_{ISD} \equiv \frac{S_{0x}-S_x(B_{ext}=0)}{S_x(B_{ext}=0)} = \frac{\left((\omega_y^{ms})^2+(\omega_z^{ms})^2\right)(\omega_L^{ms}\tau_{sf})^2}{(\omega_x^{ms})^2\left(1+(\omega_L^{ms}\tau_{sf})^2\right)+(\omega_y^{ms})^2+(\omega_z^{ms})^2}, \quad (2)$$

where $(\omega_L^{ms})^2 = (\omega_x^{ms})^2+(\omega_y^{ms})^2+(\omega_z^{ms})^2$. When $\tau_{sf} \gg 1/\omega_L^{ms}$, the R_{ISD} is determined only by the ratio of each component, $((B_y^{ms})^2+(B_z^{ms})^2)/(B_x^{ms})^2$ or $((\omega_y^{ms})^2+(\omega_z^{ms})^2)/(\omega_x^{ms})^2$.

As depicted in Fig. 3(d), the R_{ISD} is strongly enhanced at high values of τ_{sf}; when $1/\omega_L^{ms}$ is small, the R_{ISD} increases more rapidly as a function of τ_{sf}. The calculated R_{ISD} are relatively smaller than the observed values because the magnitudes of three components (B_x^{ms}, B_y^{ms}, B_z^{ms}) are assumed to be the same for simplicity.

Two important points can be obtained from the τ_{eff} vs. τ_{sf} plot with different values of $1/\omega_L^{ms}$ in Fig. 3(e) (note that the τ_{sf} is the input value for the calculation and the τ_{eff} is the extracted value from the calculated normal Hanle curve, see Figs. 3(a)–3(c)). The first point is that the τ_{eff} is significantly dependent on the $1/\omega_L^{ms}$. For example, for the small values of $1/\omega_L^{ms}$, the τ_{eff} significantly deviates from the τ_{sf}. The second one is that, in spite of the artificial broadening by B_L^{ms}, the τ_{eff} still is a monotonically increasing function of the τ_{sf}. The increase of the τ_{sf} results in the increase of both τ_{eff} and R_{ISD}. This agrees with our experimental finding that the R_{ISD} is positively correlated with the τ_{eff}. Based on the reasonable agreement of the calculated curves with observed ones, we conclude that this model basically explains the experimental finding quite well and captures the basic physics.

In conclusion, our experimental results show the role of host SC and spin lifetime on the ISD. Using the CoFe/MgO on Si and Ge contacts with a similar interfacial roughness, we have observed significant differences of the ISD depending on the host SC; the spin accumulation in different SCs exposed to the local fields from similar FMs gives rise to a clearly different ratio of the inverted Hanle signal to the normal one. The model calculation, considering the spin precession due to the local field and the spin relaxation in the host SC, reproduces the experimental observations.

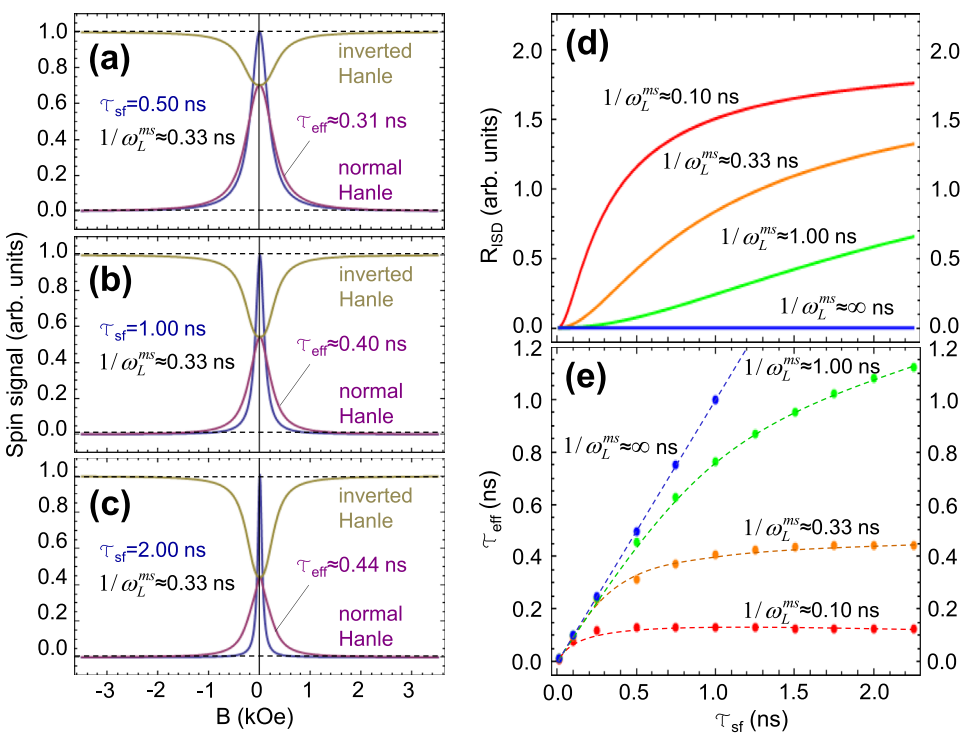

FIG. 3. (a)–(c) Calculated normal ($M\perp B$, wine symbol) and inverted ($M//B$, brown symbols) Hanle curves. The spin lifetime (τ_{sf}, blue symbols) was varied from 0.50 ns to 2.00 ns at a fixed value of $1/\omega_L^{ms}$ of about 0.33 ns, corresponding to a B^{ms} value of 0.3 kOe. The ideal Hanle curves (blue symbols) without B_L^{ms} are also presented for comparison. (d) Calculated the R_{ISD} as a function of τ_{sf} with the four different $1/\omega_L^{ms}$ values of about 0.10, 0.33, 1.00, and ∞ ns, corresponding to B_L^{ms} values of about 1.0, 0.3, 0.1, and 0.0 kOe, respectively. (e) τ_{eff} vs. τ_{sf} plot for different values of $1/\omega_L^{ms}$. It is noted that the τ_{sf} is the input value for the calculation and the τ_{eff} is the extracted value from the calculated normal Hanle curve (see (a)–(c)).

This work was supported by the National Research Laboratory Program Contract No. R0A-2007-000-20026-0 through the National Research Foundation of Korea funded by the Ministry of Education, Science and Technology, the KIST institutional program, and by KBSI Grant No. T32517 for Seung-Young Park.

[1]X. Lou, C. Adelmann, M. Furis, S. A. Crooker, C. J. Palmstrøm, and P. A. Crowell, Phys. Rev. Lett. **96**, 176603 (2006).
[2]S. P. Dash, S. Sharma, R. S. Patel, M. P. de Jong, and R. Jansen, Nature (London) **462**, 491 (2009).
[3]R. Jansen, B. C. Min, S. P. Dash, S. Sharma, G. Kioseoglou, A. T. Hanbicki, O. M. J. van't Erve, P. E. Thompson, and B. T. Jonker, Phys. Rev. B **82**, 241305(R) (2010).
[4]C. H. Li, O. M. J. van't Erve, and B. T. Jonker, Nat. Commun. **2**, 245 (2011).
[5]N. W. Gray and A. Tiwari, Appl. Phys. Lett. **98**, 102112 (2011).
[6]K.-R. Jeon, B.-C. Min, I.-J. Shin, C.-Y. Park, H.-S. Lee, Y.-H. Jo, and S.-C. Shin, Appl. Phys. Lett. **98**, 262102 (2011).
[7]Y. Ando, K. Kasahara, K. Yamane, Y. Baba, Y. Maeda, Y. Hoshi, K. Sawano, M. Miyao, and K. Hamaya, Appl. Phys. Lett. **99**, 012113 (2011).
[8]H. Saito, S. Watanabe, Y. Mineno, S. Sharma, R. Jansen, S. Yuasa, and K. Ando, Solid State Commun. **151**, 1159 (2011).
[9]K.-R. Jeon, B.-C. Min, Y.-H. Jo, H.-S. Lee, I.-J. Shin, C.-Y. Park, S.-Y. Park, and S.-C. Shin, Phys. Rev. B **84**, 165315 (2011).
[10]K.-R. Jeon, B.-C. Min, Y.-H. Park, H.-S. Lee, C.-Y. Park, Y.-H. Jo, and S.-C. Shin, Appl. Phys. Lett. **99**, 162106 (2011).
[11]A. Jain, L. Louahadj, J. Peiro, J. C. Le Breton, C. Vergnaud, A. Barski, C. Beigné, L. Notin, A. Marty, V. Baltz, S. Auffret, E. Augendre, H. Jaffrès, J. M. George, and M. Jamet, Appl. Phys. Lett. **99**, 162102 (2011).
[12]K. Kasahara, Y. Baba, K. Yamane, Y. Ando, S. Yamada, Y. Hoshi, K. Sawano, M. Miyao, and K. Hamaya, J. Appl. Phys. **111**, 07C503 (2012).
[13]A. T. Hanbicki, S. F. Cheng, R. Goswami, O. M. J. van't Erve, and B. T. Jonker, Solid State Commun. **152**, 244 (2011).
[14]M. Johnson and R. H. Silsbee, Phys. Rev. Lett. **55**, 1790 (1985).
[15]M. Johnson and R. H. Silsbee, Phys. Rev. B **37**, 5326 (1988).
[16]M. Tran, H. Jaffrès, C. Deranlot, J.-M. George, A. Fert, A. Miard, and A. Lemaître, Phys. Rev. Lett. **102**, 036601 (2009).
[17]S. P. Dash, S. Sharma, J. C. Le Breton, H. Jaffrès, J. Peiro, J.-M. George, A. Lemaitre, and R. Jansen, Phys. Rev. B **84**, 054410 (2011).
[18]See supplementary material at http://dx.doi.org/10.1063/1.4733478 for the analysis on the bias dependence of normal and inverted Hanle effects.
[19]K.-R. Jeon, C.-Y. Park, and S.-C. Shin, Cryst. Growth Des. **10**, 1346 (2010).
[20]R. S. Patel, S. P. Dash, M. P. de Jong, and R. Jansen, J. Appl. Phys. **106**, 016107 (2009).
[21]C. Gould, C. Ruster, T. Jungwirth, E. Girgis, G. M. Schott, R. Giraud, K. Brunner, G. Schmidt, and L. W. Molenkamp, Phys. Rev. Lett. **93**, 117203 (2004).
[22]H. Saito, S. Yuasa, and K. Ando, Phys. Rev. Lett. **95**, 086604 (2005).
[23]L. Gao, X. Jiang, S. H. Yang, J. D. Burton, E. Y. Tsymbal, and S. S. P. Parkin, Phys. Rev. Lett. **99**, 226602 (2007).
[24]T. Umemura, M. Harada, K. Matsuda, and M. Yamamoto, Appl. Phys. Lett. **96**, 252106 (2010).
[25]R. S. Liu, L. Michalak, C. M. Canali, L. Samuelson, and H. Pettersson, Nano Lett. **8**, 848 (2008).
[26]R. J. Elliott, Phys. Rev. **96**, 266 (1954); Y. Yafet, in *Solid State Physics*, edited by F. Seitz and D. Turnbull (Academic, New York, 1963), Vol. 14, p. 1.
[27]O. D. Restrepo and W. Windl, e-print arXiv:1010.5436v2.
[28]J. L. Cheng, M. W. Wu, and J. Fabian, Phys. Rev. Lett. **104**, 016601 (2010).
[29]W. Kipferl, M. Dumm, M. Rahm, and G. Bayreuther, J. Appl. Phys. **93**, 7601 (2003).
[30]W. Wang, H. Sukegawa, and K. Inomata, Phys. Rev. B **82**, 092402 (2010).